Article

Cytoskeletal Pinning Controls Phase Separation in Multicomponent Lipid Membranes

Senthil Arumugam,[1,2,3] Eugene P. Petrov,[4,*] and Petra Schwille[4,*]
[1]Institut Curie, Centre de Recherche, Paris, France; [2]CNRS, UMR 168, Physico-chimie Curie, Paris, France; [3]CNRS, UMR 3666, Endocytic Trafficking and Therapeutic Delivery Group, Paris, France; and [4]Max Planck Institute of Biochemistry, Department of Cellular and Molecular Biophysics, Am Klopferspitz 18, Martinsried, Germany

ABSTRACT We study the effect of a minimal cytoskeletal network formed on the surface of giant unilamellar vesicles by the prokaryotic tubulin homolog, FtsZ, on phase separation in freestanding lipid membranes. FtsZ has been modified to interact with the membrane through a membrane targeting sequence from the prokaryotic protein MinD. FtsZ with the attached membrane targeting sequence efficiently forms a highly interconnected network on membranes with a concentration-dependent mesh size, much similar to the eukaryotic cytoskeletal network underlying the plasma membrane. Using giant unilamellar vesicles formed from a quaternary lipid mixture, we demonstrate that the artificial membrane-associated cytoskeleton, on the one hand, suppresses large-scale phase separation below the phase transition temperature, and, on the other hand, preserves phase separation above the transition temperature. Our experimental observations support the ideas put forward in our previous simulation study: In particular, the picket fence effect on phase separation may explain why micrometer-scale membrane domains are observed in isolated, cytoskeleton-free giant plasma membrane vesicles, but not in intact cell membranes. The experimentally observed suppression of large-scale phase separation much below the transition temperatures also serves as an argument in favor of the cryoprotective role of the cytoskeleton.

INTRODUCTION

The plasma membranes of cells are highly heterogeneous in their lateral organization. This heterogeneity is supposedly an important parameter in regulating various biologically relevant processes. Model membranes have been widely used to understand the behavior of cellular membranes. However, being minimalistic and oversimplified, model membrane systems cannot fully capture the behavior of a complex biological membrane (1). A significant shortcoming is that most model membranes are being studied without considering the effects of membrane-associated cytoskeleton. Large-scale phase separation, which is easily observable in model membrane systems, has been elusive in cell membranes. If, however, the biological membrane is isolated from the cell, the phase separation with lipid domains on the micrometer scale can easily be observed. This is the case, for example, for giant unilamellar vesicles (GUVs) made of yeast lipid extracts (2) and giant plasma membrane vesicles (3,4). Additionally, these plasma membrane-derived vesicles begin to show macroscopic phase separation at temperatures substantially below 37°C (4). These membranes have nearly the same lipid composition as the corresponding cell membranes except largely lacking the PI(4,5)P_2 (5); however, they are devoid of any cytoskeletal elements associated with them.

Recent Monte Carlo (MC) simulations of lipid membranes (6,7) have demonstrated that phase separation and lateral diffusion in membranes can be strongly affected by the interaction with membrane-associated cytoskeleton or protein obstacles. (For discussion of theoretical work on the effect of cytoskeleton and immobile proteins on phase separation in membranes, see the recent review (8)). It has been shown using simulations that, due to interaction of the membrane with the cytoskeleton, the lipid domains lose their mobility and mostly stay pinned to the cytoskeleton. The size and geometry of lipid domains are determined by the interplay of the cytoskeleton mesh size and membrane composition. As a result, interaction with the cytoskeleton prevents large-scale phase separation in the membrane. It has been suggested that these findings can explain why micrometer-scale membrane domains are observed in isolated, cytoskeleton-free giant plasma membrane vesicles, but not in intact cell membranes; additionally, a microscopic picture of the cryoprotective role played by the cytoskeleton was offered (6).

The complex nature of interactions involving multiple components of actin-binding proteins makes it extremely complicated to mimic and tune a picket fence system on the membrane in in vitro experimental systems. Nevertheless, several attempts in this direction have been made, and their results generally agree with the conclusions based on computer simulations. It has been shown that association of the dendritic actin cytoskeleton to phosphatidylinositol-containing three-component lipid membranes capable of exhibiting

Submitted May 28, 2014, and accepted for publication December 23, 2014.
*Correspondence: schwille@biochem.mpg.de or petrov@biochem.mpg.de
Editor: Tobias Baumgart.

0006-3495/15/03/1104/10 $2.00
http://dx.doi.org/10.1016/j.bpj.2014.12.050

liquid-ordered and liquid-disordered (L_o-L_d) phase coexistence via phosphatidylinositol 4,5-bisphosphate binding proteins increases the temperature of miscibility and affects organization of lipid domains (9), suggesting that cytoskeletal pinning may stabilize heterogeneities at temperatures much above the miscibility temperature. However, in this experimental system, the actin filaments did not form a stationary network that would suppress large-scale phase separation in the membrane, but, rather, the spatial arrangement of actin filaments followed that of domains in the phase-separating membrane. Using a simplified approach of linking the actin cortex to the membrane by neutravidin and biotinylated lipids, it was found that the cytoskeleton reduces the lateral diffusion of lipids and protein molecules in the bilayer (10). To focus on the general features of the membrane-cytoskeleton interaction and avoid potential artifacts, we chose to study the effect of an alternative, non-actin-based filament network on phase separation in freestanding lipid membranes. During the preparation of this manuscript on results we have presented previously (11), a new experimental and simulation study on the interaction of artificial actin network with supported lipid membranes was published (12), which combined the above-mentioned method of linking actin to the membrane using biotin-neutravidin interactions with phase separating lipid compositions. However, the properties of supported lipid bilayers can be strongly influenced by the interaction with the solid support (13,14), which can considerably complicate the interpretation of experimental results. While confirming the earlier theoretical and experimental findings about the influence of the filament network on lipid diffusion, the study (12) put an emphasis on the importance of local deformations of the membrane by the attached actin network. It is, however, rather unlikely that the membrane, which is strongly attached to a flat solid support, would undergo a considerable deformation as a result of interaction with an actin filament.

In this article, using an alternative system consisting of freestanding membranes and non-actin-based filament network, we demonstrate experimentally the effect of a cytoskeletal pinning on phase separation and coexistence in freestanding multicomponent lipid membranes, and compare our experimental results with our MC simulations.

The cytoskeletal element we employ in this work is FtsZ protein, a tubulin homolog from prokaryotes, which has been previously shown to polymerize into dense polymer networks on GUVs and supported lipid membranes (15,16). The physical nature of the network is similar to those seen in eukaryotic membranes—with multiple branching and compartmentalization. As a model of freestanding lipid membrane showing phase coexistence, we employ GUVs made of a quaternary lipid mixture.

Using this experimental system, we demonstrate that:

1. FtsZ filaments bind to the L_d phase of freestanding phase-separated lipid membrane and form a polymer network attached to the membrane surface.
2. The network of membrane-bound FtsZ filaments on the one hand, prevents large-scale L_o-L_d phase separation at lower temperatures and on the other hand, preserves the phase coexistence at higher temperatures compared to a free membrane.
3. The size of L_o-phase domains formed in the presence of FtsZ filaments is controlled by the size of the voids of the filament network.
4. On removal of the filament network, smaller L_o domains become mobile and coalesce readily to form larger domains.
5. By MC simulations with a simple minimalistic two-component membrane system interacting with a cytoskeleton, we manage to reproduce all the key findings observed in the experiments, thereby showing that the phenomenon is general and does not depend on particular details of the system.

MATERIALS AND METHODS

FtsZ purification and assembly

A chimeric version of FtsZ, FtsZ-YFP-MTS, was used for the experiments. It consists of *Escherichia coli* FtsZ with a copy of yellow fluorescent protein (YFP) fused to the amino acid 366 of the C-terminal of FtsZ, followed by a membrane targeting sequence (MTS) from MinD (a protein from *E. coli* divisome). *E. coli* FtsZ-YFP-MTS was purified as described elsewhere (17). Briefly, FtsZ-YFP-MTS was expressed from pET11b vector in BL21 cells. Cells were lysed by sonication in TRIS buffer (50 mM TRIS, 1 mM EDTA, 50 mM KCl, and 10% glycerol), and FtsZ-YFP-MTS was precipitated from the supernatant by 40% ammonium sulfate. After that it was resuspended, dialyzed against TRIS buffer, further purified using a Resource Q anion exchange column (Amersham Biosciences, Piscataway, NJ), desalted, and stored in aliquots in TRIS buffer.

Preparation of GUVs decorated with an FtsZ network

1,2-dioleoyl-*sn*-glycero-3-phosphocholine (DOPC), 1,2-dioleoyl-*sn*-glycero-3-phospho-*rac*-(1-glycerol) (DOPG), cholesterol (Chol), and chicken egg yolk sphingomyelin (eSM) were purchased from Avanti Polar Lipids (Alabaster, AL). Fast DiI was purchased from Life Technologies GmbH (Darmstadt, Germany). DSPE-PEG-KK114 was a kind gift from Christian Eggeling, University of Oxford, UK. GUVs were prepared by electroformation as described elsewhere (18). To this end, 1 μl of DOPC/DOPG/eSM/Chol at 2.5:2.5:3:2 ratio at 1 mg/ml in chloroform was spread on two parallel Pt wire electrodes placed 4 mm apart. The electrodes with the lipid film were immersed in a chamber containing 320 mM sucrose solution in MilliQ water and were connected to an AC voltage source. Electroformation was performed at 2 V (rms) and 10 Hz for 1 h at 65°C. GUVs were released from the electrodes by changing the frequency to 2 Hz for 30 min. Separately, the observation chamber was prepared in the following way: To prevent adhesion of the GUVs to the inner surfaces of the chamber, the surfaces were coated with bovine serum albumin (BSA) by filling the chamber with BSA (1 mg/ml) solution, which after 30 min was washed twice and filled with glucose solution having the same osmolarity as the glucose solution used for GUV electroformation. The GUVs were then transferred into the chamber and sank to its bottom as a result of the difference in densities of the glucose and sucrose solutions. Half the volume of glucose-sucrose solution was removed and replaced by polymerization

buffer (50 mM MES, 50 mM KCl, 15 mM $MgCl_2$, pH 6.5, osmolarity adjusted to 320 mOsm/kg by adding glycerol). FtsZ-YFP-MTS was polymerized on the GUVs at a final concentration of 1 μM FtsZ-YFP-MTS and 0.5 mM guanosine-5′-[(α,β)-methyleno]triphosphate (GMPCPP). It has been shown that by changing the bulk concentration of FtsZ, one can vary the density of the FtsZ meshwork on the membrane (16). Lower concentrations of 0.5 μM were used with 7.5 mM Ca^{2+}, which induces FtsZ bundling (19) to produce networks with large mesh sizes. In experiments with MinC, GMPCPP was replaced with GTP at a concentration of 1 mM.

Fluorescence imaging

Fluorescence imaging was performed with an LSM 710 laser scanning microscope equipped with a C-Apochromat 40× 1.2 NA objective (both from Carl Zeiss, Jena, Germany). YFP was excited at 488 nm, and fluorescence was detected using a 505–530 nm emission filter. Membrane labeling dye Fast DiI was excited at 543 nm, and its emission was detected through an LP 560 nm filter. In cases where DSPE-PEG-KK114 was used, the Fast DiI emission was collected through a 560–620 nm band pass filter. Fluorescence of DSPE-PEG-KK114 was excited at 633 nm and collected using an LP 650 nm filter (20).

Temperature control

The temperature control (heating and cooling) was achieved in the sample chamber using a CL100 Peltier based system (Warner Instruments, Hamden, CT). The chamber was prepared from a cut pipette tip glued to the coverslip using UV glue (Norland optical adhesive 61, Norland Products, Cranbury, NJ). An outer plastic ring was glued to the same coverslip. The inner chamber was used for the sample. The outer area was filled with mineral oil, which helped distribute the heat. The heating/cooling rates were 1°C/min. During the measurements, every time the temperature was changed, the system was left to equilibrate for 30 min.

Image analysis

Areas of membrane domains and the corresponding FtsZ network mesh sizes were determined for GUVs with radii in the range of 2.5–14.4 μm using the upper pole of the vesicles to minimize the effects of the vesicle curvature. In case of small domains (<5 μm in diameter) the areas were determined using the Measure plugin for ImageJ software (http://rsbweb.nih.gov/ij/). For larger domains that extended beyond a single focal plane, a three-dimensional image was created from a stack of confocal images at different z positions using the volume viewer plugin for ImageJ and analyzed using the isosurface function in boneJ (21). Corresponding total areas of GUVs were estimated using their equatorial radii under the assumption of their spherical shape.

MC simulations

MC simulations were carried out using the approach we have presented previously (22). In short, MC simulations were carried out on a 400 × 400 square lattice with periodic boundary conditions, where every cell of the lattice represents one of the two lipids. In the simulation, the lipid ratio is kept fixed. In this simulation of a binary lipid system, each of the lipids can exist in two conformations, which correspond to the gel and fluid phase. These conformational transitions are thermally driven, and therefore the relative amount of the gel and fluid phase is conserved only on average. Additionally, the lipids can exercise translational motion on the lattice by means of the next-neighbor exchange. The energetics of the lipid-lipid interaction is adjusted to reproduce the excess heat capacity profiles of a particular lipid mixture. For details of the implementation of the algorithm and the choice of the simulation parameters, see (6,22).

By assuming the average headgroup size of 0.8 nm, our lattice corresponds to a membrane patch of 0.32 × 0.32 μm^2. The size of the membrane is thus large enough to clearly separate the effects of true phase separation from thermally driven microscopic fluctuations (22). The cytoskeleton was modeled, as previously (6), using a random Voronoi tessellation satisfying the periodic boundary conditions with the average size of the mesh of 66.6 lattice units, which corresponds to ~53 nm. The filament meshwork generated by this approach is projected on the square lattice, which results in a set of pixels representing the locations on the filaments. Based on the geometry of the FtsZ filaments, 25% of these pixels are assigned to be the pinning sites of the meshwork. Because the membrane-targeting sequence employed in our experiments shows a strong preference for the L_d phase (vide infra), the following rule was selected for the membrane-cytoskeleton interaction in our simulations: A lipid located at the given moment at a filament pinning site is forced to assume a fluid (L_d) conformation with no restrictions on its mobility. (This is in contrast with our previous simulation work (6), where it was assumed that the pinning sites of the membrane skeleton exert the aligning, rather than disordering, effect on lipid tails.)

RESULTS

FtsZ-YFP-MTS preferentially binds to the L_d phase of lipid bilayer

The binding moiety of each FtsZ monomer is an artificially linked MTS that is originally derived from *E. coli* protein MinD. The MTS is a transplantable amphipathic helix—KGFLKRLF—that displays a unique cooperativity in binding to negatively charged membranes: When in monomeric form, it has a moderate affinity to the membrane, whereas in dimeric or higher oligomeric forms, it has a very strong affinity to the membrane (23,24). Being an amphipathic helix, it only inserts into the outer leaflet of a bilayer. Typically, amphipathic helices must have strong affinities for the L_d phase, which favors their insertion into the membrane. Therefore, the MTS being on each monomer of the FtsZ polymeric network are expected to act as nucleation centers for L_d domains in the lipid membrane. With FtsZ-YFP-MTS, the polymeric network can be easily visualized using fluorescence microscopy (15–17).

To take advantage of the properties of the canonical raft mixture and at the same time to ensure MTS binding (which requires negatively charged lipids), in this study we chose to work with a quaternary lipid mixture DOPC/DOPG/eSM/Chol. Additionally, we exploited the fact that DOPG has the same acyl chains as DOPC, resulting in very similar thermal behavior. In the DOPC/eSM/Chol lipid mixture, the boundary between the L_o phase and L_o and L_d phase coexistence is crossed close to the composition of 6:2:2 at 25°C (25) if one moves on the ternary phase diagram along the Chol line. On the other hand, the DOPG/eSM/Chol lipid mixture has been shown to exhibit L_o and L_d fluid phase coexistence at the composition of 3:5:2 at 23°C (26). We therefore expected a similar behavior from a quarternary system where 50% of DOPC is replaced by DOPG. By sampling along the Chol line of the phase diagram of the quarternary lipid mixture DOPC/DOPG/eSM/Chol with equal concentrations of DOPC and DOPG, we found that the lipid

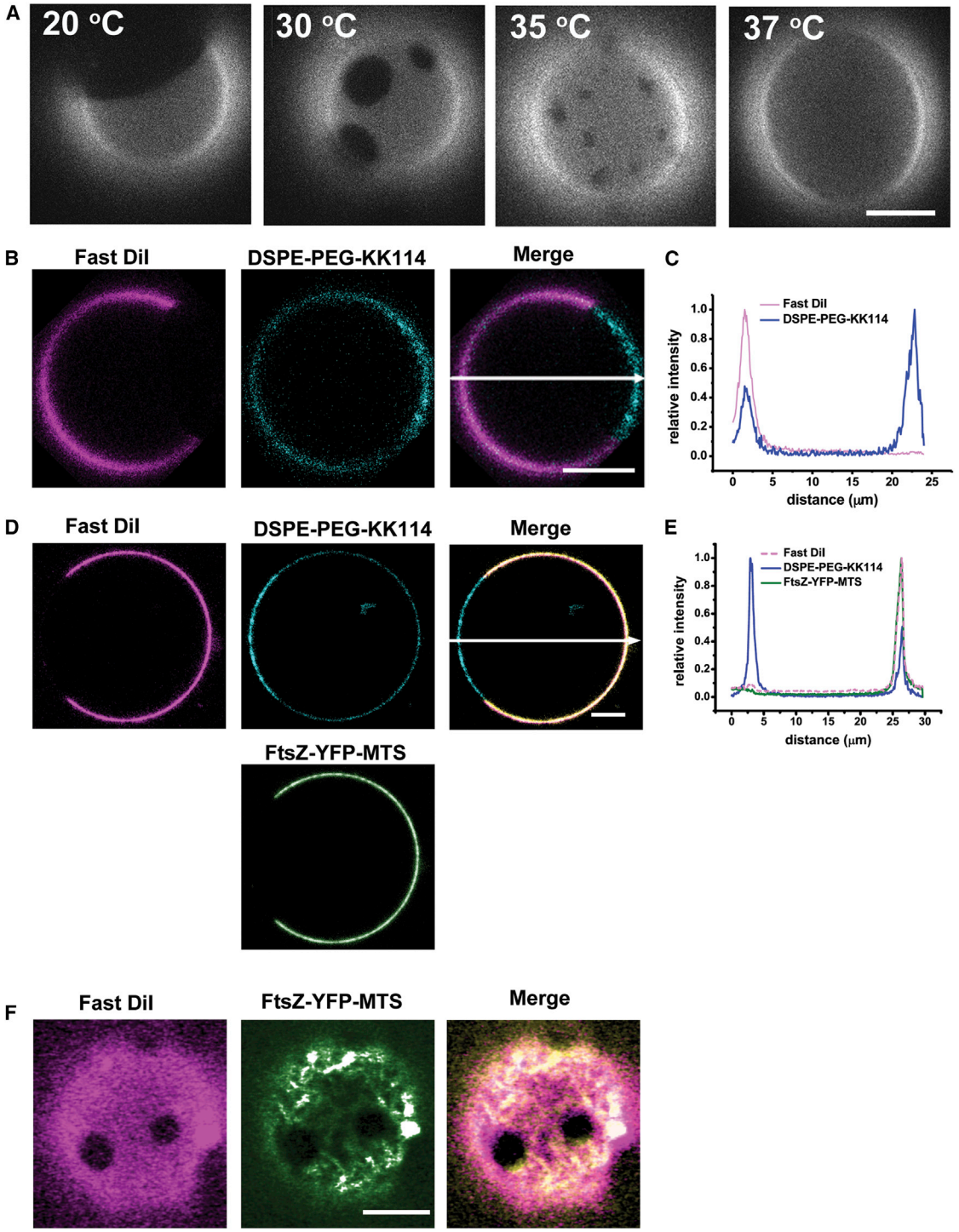

FIGURE 1 FtsZ-YFP-MTS localizes to L_d domains. (*A*) Vesicles composed of DOPC/DOPG/eSM/Chol at 2.5:2.5:3:2 at various temperatures. At 37°C, the membrane is homogeneous. (*B*) Partitioning of L_o marker (DSPE-PEG-KK114) and L_d marker (Fast DiI). (*C*) Intensity profile across the GUV shown in (*B*). (*D*) FtsZ-YFP-MTS binds exclusively to the L_d phase marked by Fast DiI and avoids the L_o phase marked by DSPE-PEG-KK114. (*E*) Intensity profile across the GUV shown in (*D*). (*F*) FtsZ-YFP-MTS meshwork localizes to the L_d phase marked by Fast DiI. Temperature (*B–F*): 25°C. Scale bars: 10 μm. To see this figure in color, go online.

mixture with the composition of 2.5:2.5:3:2 exhibits a homogeneous L_o phase at 37°C and above, and undergoes a transition to L_o-L_d phase coexistence at lower temperatures with the transition temperature estimated to be between 36 and 37°C (Fig. 1 *A*). All experiments discussed in this work were carried out using this lipid mixture.

To visualize the L_o and L_d domains in our membranes, we employed previously established fluorescent markers—Fast DiI to visualize the L_d phase and DSPE-PEG-KK114 to visualize the L_o phase (Fig. 1, *B* and *C*) (3,20,25). We find that a mixture of DOPC/DOPG/eSM/Chol at 2.5:2.5:3:2 displays L_o-L_d phase coexistence, characterized by presence of round L_o domains (Fig. 1 *A*). The quaternary mixture shows a phase transition temperature of 36°C in the absence of bound filaments (the same picture is observed for GUVs very sparsely coated with filaments resulting in very large mesh sizes).

On adding FtsZ-YFP-MTS to the vesicles in the absence of GTP or GMPCPP, we observe no binding, as has been previously reported for monomeric MTS. On addition of either GTP or GMPCPP, the filaments start to polymerize and assemble on the vesicles. In all cases where filament polymerization takes place on vesicles already showing L_o-L_d phase separation, the filaments bind exclusively to the L_d phase and settle into an interconnected network (Fig. 1, *D–F*). The MTS is inserted into the outer leaflet of the membrane in the L_d phase (Fig. 2). We observed that for experiments with varying temperatures, filaments assembled with GMPCPP were much more stable compared to those assembled with GTP. We confirmed that the general organization of the FtsZ filament meshwork assembled with GMPCPP does not change with temperature (Supporting Material and Fig. S1). The stability of the filaments assembled with GMPCPP is likely due to the inhibition of hydrolysis-dependent turnover of FtsZ monomers in the filaments.

Compartmentalization of the membrane prevents large-scale phase separation

To study the effect of cytoskeletal pinning on phase separation and formation of large domains, we used the mixture of DOPC/DOPG/eSM/Chol at 2.5:2.5:3:2 with FtsZ-YFP-MTS assembled with GMPCPP.

The temperature-dependent behavior of the free membrane without a protein meshwork is illustrated by snapshots shown in Fig. 1 *A*. At 37°C, above the phase transition temperature of the four-component membrane, the membrane is in the L_d phase and thus shows a uniform structure. As expected, upon cooling below the phase transition temperature, L_o domains start to form and coalesce.

To study the effect of the artificial cytoskeletal meshwork on phase separation in the lipid membranes, FtsZ-YFP-MTS was first polymerized on GUVs prepared with the quaternary mixture described previously at a temperature of 25°C at which GUVs typically show several domains of the L_o phase. In this case, the FtsZ network is formed only on the L_d phase, whereas the L_o domains remain free from the artificial cytoskeleton. After the FtsZ network was formed, observations were carried out while the sample was slowly heated in steps of 2°C over 1.5 h to reach 41°C, after which the sample was slowly cooled for 2 h down to 20°C (Fig. 3). At the temperatures exceeding 36°C, no phase separation is observed in the free membrane (Fig. 1). At the same time, the membrane decorated with the FtsZ meshwork (with a mesh size of 2–5 μm^2) still preserves phase coexistence at 39°C (Figs. 3 and 4 *A*), which means that membrane interaction with the artificial cytoskeleton suppresses the melting transition. The fact that melting of L_o domains is inhibited in the presence of the cytoskeletal network is also reflected by the percentage of phase-separated vesicles at a certain temperature compared to the free membrane (Fig. 4). When the membrane is cooled down to 25°C, the L_o domains are formed only within the voids of the meshwork and show neither lateral motion, nor coalescence. Remarkably, when the membrane is further cooled down to 20°C, the L_o domains either do not grow or grow insignificantly, or do not show coalescence even after 2 h (Figs. 3 and 4 *B*).

We point out that inhibition of domain melting at higher temperatures and of domain coalescence at lower temperatures by the cytoskeleton only takes place if the cytoskeletal network has a large enough density. When the network is too coarse (typical mesh area larger than ~25 μm^2), upon heating above the phase coexistence temperature, the domains melt at a temperature similar to the naked vesicles and, upon cooling below the phase coexistence temperature, large domains are formed (Fig. 5).

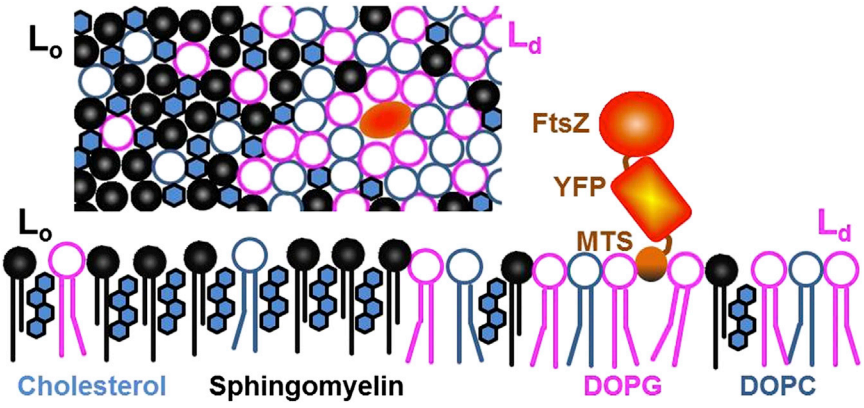

FIGURE 2 Quaternary lipid system with FtsZ-YFP-MTS binding to the L_d phase. To see this figure in color, go online.

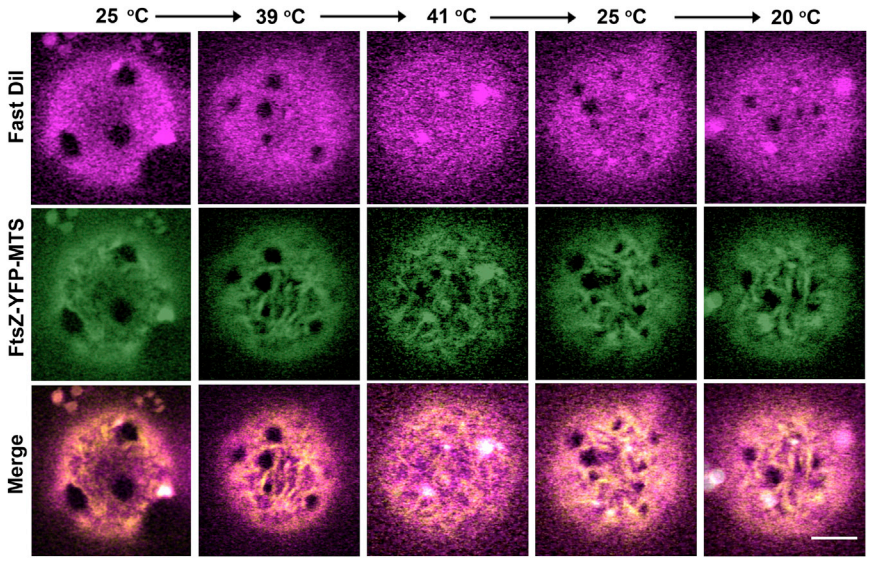

FIGURE 3 Effect of FtsZ meshwork on phase separation: Presence of dense FtsZ meshwork increases the phase transition temperature and inhibits growth of larger domains at temperatures much below phase transition temperatures. Note that the GUV is not immobilized and moves and reorients between the images corresponding to the different temperatures. Scale bar: 5 μm. To see this figure in color, go online.

We find that in the case of dense FtsZ networks on the membrane (typical mesh area smaller than ~25 μm^2) the domain sizes and shapes follow those of the meshes of the FtsZ network (Fig. 6, *A* and *B*). For large mesh sizes (mesh area larger than ~25 μm^2), the domain size is still restricted by the filament network (Fig. 6 *A*), but the domains acquire rounded shapes (Fig. 6 *C*). We believe that the phenomenon is a competition between the energies of wetting of filaments by the L_d phase and line tension between the L_o and L_d phases. One should expect that for a dense network, the wetting energy wins, most of the L_d phase is condensed on the filaments, and domains follow meshes in size and shape. On the other hand, for sparse network, there is a considerable fraction of the L_d phase, which is not associated with the network; as a result, the line tension energy is expected to dominate, and domains, whose sizes are still restricted by the network, attain rounded shapes.

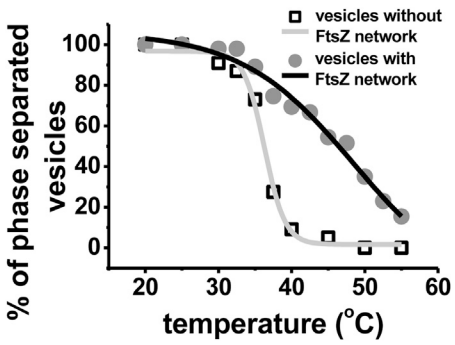

FIGURE 4 FtsZ meshwork increases the temperature range for membrane phase coexistence. Percentage of vesicles displaying phase separation in the presence and absence of FtsZ meshwork at different temperatures. Presence of cytoskeleton increases the temperature of miscibility for the membrane. Curves are drawn as a guide for the eye.

The shapes of domains in the presence of the cytoskeleton on the membrane are also influenced by the stiffness of filaments forming the meshwork and the line tension at the boundary of the lipid phases. In the presence of a dense network made of very stiff filaments the domain shape is expected to mimic that of the mesh void. On the other hand, in the case where filaments are flexible enough, one can expect that the line tension dominates, and the domain assumes a circular shape by deforming and pushing away the filaments constituting the meshwork. Our experimental system allows us to test this experimentally. If MinC, an *E. coli* protein that depolymerizes the FtsZ network assembled on bilayers in vitro (16), is added at a ratio [MinC]/[FtsZ] $\approx$ 0.4, the filaments become more flexible. Previous studies investigating the effect of MinC on the flexibility of FtsZ filaments (27) show that in the presence of MinC the persistence length of FtsZ filaments is decreased ~2.5 times from 180 to 80 nm. In this case, one can expect that at this decreased persistence length of filaments, line tension of the membrane domain will be able to overcome the filament stiffness. As a result, the meshwork around the domain is expected to deform, to adjust to a more circular domain shape.

To illustrate this point, we start with a GUV decorated with an FtsZ meshwork, which shows L_o domains having initially irregular and elongated shapes determined by the shape of meshwork voids (Fig. 7 *A*). However, upon addition of MinC at a concentration of [MinC] = 0.4 μM, [MinC]/[FtsZ] $\approx$ 0.4, the filaments reduce their rigidity, the line tension dominates, and the domains tend to attain a circular shape, minimizing line tension energy and forcing the mesh also to assume a circular shape (Fig. 7 *B*).

As demonstrated above, interaction with the cytoskeleton strongly affects the domain growth characteristics in

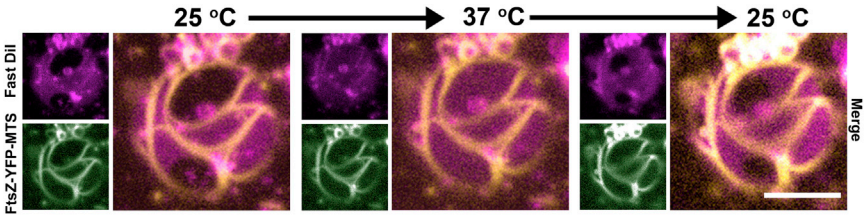

FIGURE 5 Presence of sparse FtsZ network has no effect on the phase transition temperature. Scale bar: 10 μm. To see this figure in color, go online.

the membrane. To additionally illustrate that the effect is due to the intact cytoskeleton, we use MinC to disassemble the filament meshwork on the GUV, thereby reverting it to the state of a free membrane. On adding MinC to FtsZ-coated GUVs at approximately the same concentration as the original bulk concentration of FtsZ ([MinC] = 1.0 μM, [MinC]/[FtsZ] = 1.0), the filaments are removed in ~30 s. The domains, whose sizes were previously restricted by the cytoskeletal meshwork, start to move and coalesce to form larger domains in a few minutes (Fig. 8, *A*–*C*).

MC simulations

The goal of this work is to use a minimalistic model system to study the effect of the cytoskeleton on phase separation in lipid membranes. We employ the same minimalistic approach also in our MC simulations. In particular, instead of modeling the behavior of the quaternary lipid system used in our experiments in full detail, we employ a much simpler two-component lattice-based model, which was previously demonstrated to adequately describe the phase diagram, phase separation dynamics, and diffusion in two-component lipid membranes (6,22). This binary lipid system consisting of two lipids (whose thermodynamic parameters and energetics of interaction correspond to the lipid pair of DMPC, dimyristoyl phosphatidylcholine, and DSPC, distearoyl phosphatidylcholine) will be used here as a simple minimalistic model for demonstration of the effect of the cytoskeleton on the phase separation. The purpose of the simulations presented here is to demonstrate at the conceptual level that the cytoskeleton-assisted phase separation is a very general phenomenon whose main features do not depend on the molecular details of the system. Therefore, in this sense the simulations carried out here for a two-component lipid membrane exhibiting fluid-gel (L_d-solid ordered) phase coexistence (which is not exactly the same as the quaternary lipid system exhibiting L_d-L_o phase coexistence) are relevant for understanding the main features of the phenomenon.

The phase diagram of the binary lipid system used in our simulations is shown in Fig. 9 *A*. At higher temperatures, the system is in the fluid (L_d) state. At low temperatures, the system is in the gel (solid ordered) state. At a range of intermediate temperatures, the system exhibits coexistence of the gel and fluid phases. An important property of this system is that, depending on the lipid ratio, the phase transitions from the fluid state to the fluid-gel coexistence can have a different character. At the lipid composition of DMPC/DSPC 20:80 the system has a critical point characterized by the temperature T_c = 320.5 K (6,22). As a result, in the vicinity of this point the transition from the fluid state to the fluid-gel coexistence proceeds in a continuous manner, via near-critical fluctuations. On the contrary, away from the critical composition, the character of the transition changes, and the system exhibits an abrupt phase transition (for more details, see (6,22)).

Because both types of phase transitions can be observed in more complex ternary and quaternary lipid mixtures, it seems feasible to study the effect of the cytoskeleton on the phase separation in both phase transition regimes. The results of our simulations for these two cases in the absence and in the presence of a membrane cytoskeleton depicted in Fig. 9 *C* are presented in Fig. 9, *D* and *E*. Here, by carrying out a set of simulations for a range of temperatures in the vicinity of the corresponding phase transitions for two different membrane compositions close and away from the

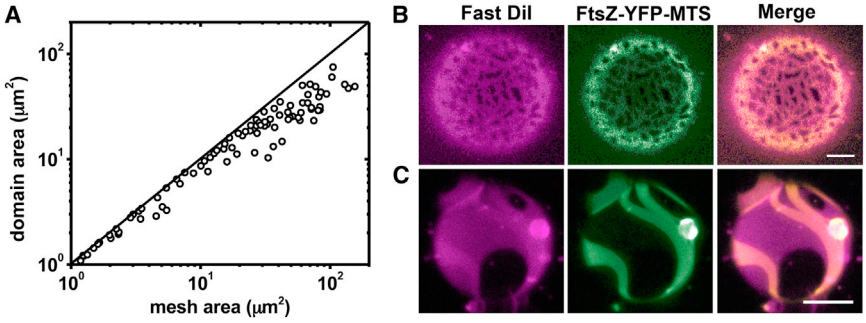

FIGURE 6 Effect of the mesh size of the FtsZ network on the character of phase separation in the membrane. (*A*) L_o domain size as a function of the mesh size of the network formed by the FtsZ-YFP-MTS (*symbols*). The dependence $y = x$ is shown as a guide for the eye (*solid line*). (*B* and *C*) Examples of the effect of dense (*B*) and sparse FtsZ network (*C*) on the domain sizes and shapes. Temperature: 25°C. Scale bars: 10 μm. To see this figure in color, go online.

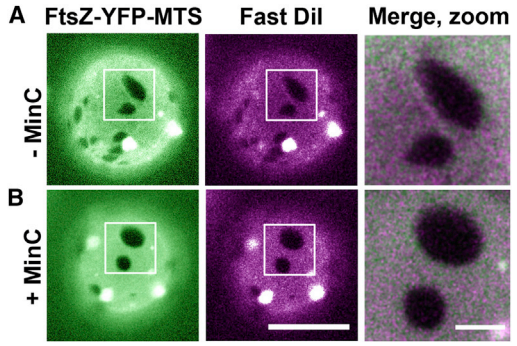

FIGURE 7 The effect of meshwork geometry and filament stiffness on domain shape. (*A*) Elongated voids result in similarly shaped domains. (*B*) Upon addition of small amounts of MinC, ([MinC] = 0.4 μM, [MinC]/[FtsZ] $\approx$ 0.4), which reduces the stiffness of the filaments, domains attain a round shape (see text for discussion). The images in the rightmost column show the enlarged view of the region of interest marked with the white square. Temperature: 25°C. Scale bar: 10 μm. To see this figure in color, go online.

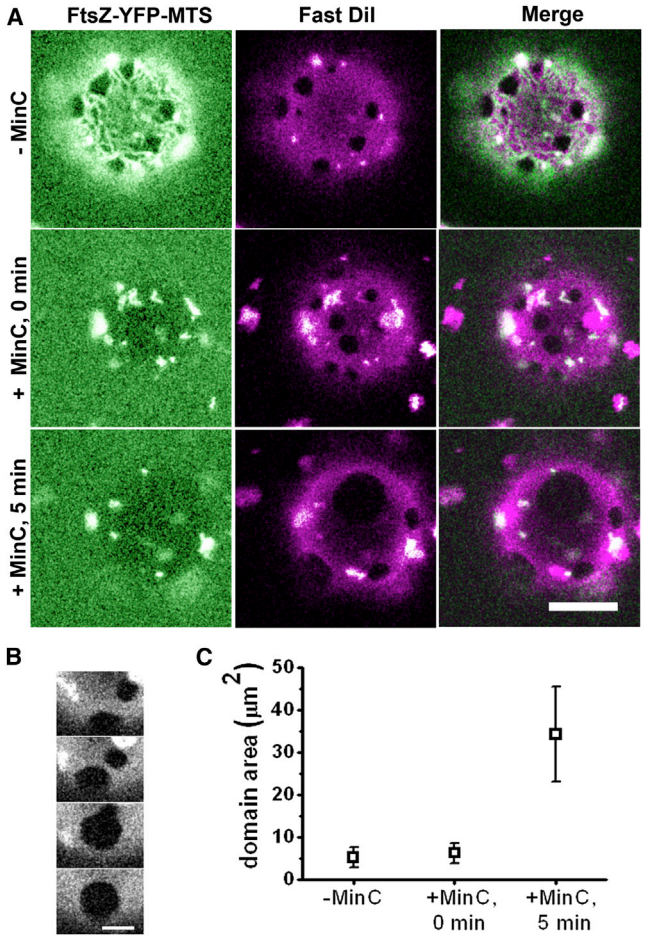

FIGURE 8 Effect of removal of the FtsZ filament network on phase separation in the membrane. (*A*) Confocal image of a pole of GUV showing assembled filaments as well as phase separation (*top*). On addition of MinC ([MinC] = 1 μM, [MinC]/[FtsZ] $\approx$ 1), a depolymerase for FtsZ, the filaments are removed from the GUV, as seen by the absence of fluorescence on the GUV. Immediately after the removal of the FtsZ network, the domains become mobile, but their size is initially the same as in the presence of filaments. Mobile domains then start to coalesce and 5 min later, large domains are formed on naked GUVs. (*B*) A time-lapse montage showing coalescence of domains upon removal of filaments by MinC. (*C*) Average domain size before and after addition of MinC. This graph represents data from 5–10 domains observed on each of 10 different vesicles. Scale bars, (*A*) 10 μm (*B*) 3 μm. To see this figure in color, go online.

critical point, we demonstrate the different characters of phase separation in the free membrane and the membrane interacting with a membrane skeleton. We see that the interaction with the cytoskeleton prevents large-scale phase separation when the system is cooled below the phase transition temperature (Fig. 9 *D* and *E*). Moreover, when the system is close to criticality (Fig. 9 *E*), the interaction with the cytoskeleton preserves the phase separation in the membrane when the latter is heated above the phase coexistence temperature. Thus, the results of the simulations show a good qualitative agreement with our experimental observations.

DISCUSSION

The results presented here clearly demonstrate the major effects of associated cytoskeleton on the phase separation in lipid membranes. We have established a minimal in vitro model of membrane cytoskeleton using FtsZ, a single filament-forming protein, which settles into a network when attached to the membranes. A proper choice of a four-component lipid mixture containing an anionic lipid and exhibiting L_o-L_d phase separation at the room temperature allowed us to study the effect of the artificial membrane-associated cytoskeleton on phase separation in the membrane. Our minimal membrane-cytoskeleton system is analogous to the complex actin/spectrin meshwork associated with cellular membranes, but reduced to the very essentials of a phase separating membrane and attached polymer meshwork. The FtsZ-based cytoskeletal system, due to its inherent nature of branching and establishing a mesh is able to maintain a filament network uniformly over the GUV membrane at all temperatures. Moreover, depolymerases like MinC can be used to remove/manipulate this cytoskeleton without disrupting membrane integrity. Thus, the approach described in this study offers a very useful minimalistic system (one filament-forming protein, four lipid molecules) capable of reproducing predicted behavior of phase separation in cellular membranes.

Our experiments show that the membrane-associated cytoskeleton prevents large-scale domain formation in membranes, and that the typical domain size is controlled by the underlying meshwork. This experimentally confirms the conclusions based on MC simulations that effectively, cytoskeletal pinning in cellular membranes may nucleate lipid microdomains and maintain the microscopic heterogeneity of the membrane even away from criticality (6). Our experiments also strongly argue for the cryoprotective role of the cytoskeleton in cells previously suggested based on

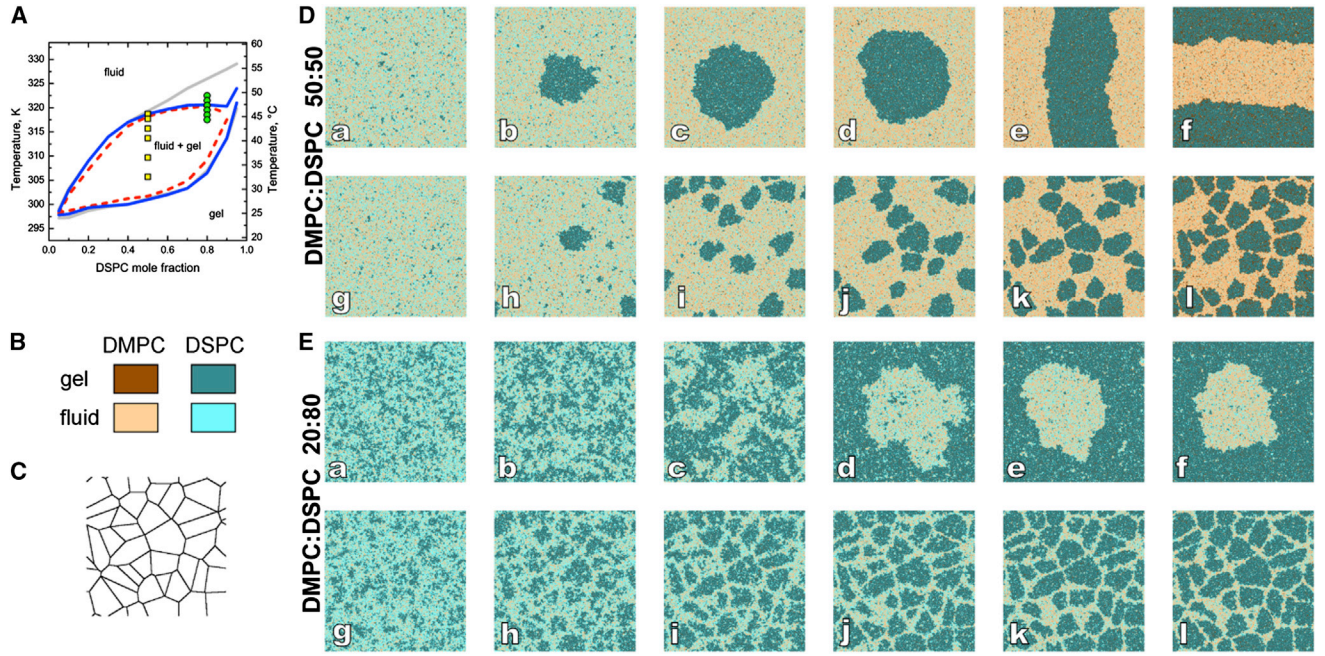

FIGURE 9 MC simulations of a two-component lipid membrane in the absence and presence of a membrane skeleton: (*A*) Phase diagram of DMPC/DSPC lipid membrane (adopted from (6)). Lipid state binodal (*solid blue curves*), lipid state spinodal (*dashed red curves*), and lipid demixing curves (*gray solid curves*) (for definition and discussion, see (6)). The critical point is located at the critical composition DMPC/DSPC 20:80 and the critical temperature $T_c = 320.5$ K. Symbols on the graph denote the temperatures and lipid compositions for which MC simulations were carried out in this work and presented in (*D*) and (*E*). (*B*) Color codes representing the lipids and their conformational states on the lattice. (*C*) Geometry of the network of filaments interacting with the membrane in simulations. The fraction of sites along the filaments, which interact with the membrane (network pinning density) is 25%. (*D*) Effect of the cytoskeleton on the phase separation in the lipid membrane with the composition exhibiting an abrupt phase transition from the L_d (*fluid*) state to the L_d-solid ordered (*fluid-gel*) coexistence. The lipid composition is DMPC/DSPC 50:50. The corresponding transition temperature is $T_t = 318.7$ K. Images (*a–f*) and (*g–l*) correspond to the free membrane and membrane interacting with the cytoskeleton, respectively. Simulations were carried out at the following temperatures: $T = T_t$ (*a*, *g*), $T = T_t - 1$ K (*b*, *h*), $T = T_t - 3$ K (*c*, *i*), $T = T_t - 5$ K (*d*, *j*), $T = T_t - 9$ K (*e*, *k*), and $T = T_t - 13$ K (*f*, *l*). (*E*) Effect of the cytoskeleton on the phase separation in the lipid membrane with the composition exhibiting a continuous phase transition from the L_d (*fluid*) state to the L_d-solid ordered (*fluid-gel*) coexistence via a critical point. The lipid composition is DMPC/DSPC 20:80. The temperature is $T_c = 320.5$ K. Images (*a–f*) and (*g–l*) correspond to the free membrane and membrane interacting with the cytoskeleton, respectively. Simulations were carried out at the following temperatures: $T = T_c + 2$ K (*a*, *g*), $T = T_c + 1$ K (*b*, *h*), $T = T_c$ (*c*, *i*), $T = T_c - 1$ K (*d*, *j*), $T = T_c - 2$ K (*e*, *k*), and $T = T_c - 3$ K (*f*, *l*). To see this figure in color, go online.

simulation results—it suppresses large-scale phase separation and maintains the heterogeneity needed by the plasma membrane to be functional at temperatures well below the phase transition temperatures. On the other hand, our experiments have shown that interaction with the cytoskeleton maintains the phase separation in the membrane also above the transition temperature, which may be important for proper functioning of the cell membranes under hyperthermic conditions.

The condensation of a particular phase along the filament should affect the character of lipid diffusion in the membrane under these conditions. Previously (6), we have shown that interaction of phase-separating lipid membrane with a cytoskeleton that favors a more viscous phase leads to hop diffusion of lipid molecules preferentially partitioning into the more fluid phase. On the other hand, if, as in the present situation, cytoskeletal filaments induce precipitation of the less viscous phase, lipid molecules preferentially partitioning into this phase should move predominantly along the filaments, as has been demonstrated recently (12). One should expect that in fluorescence correlation spectroscopy measurements under these conditions this quasi-one-dimensional diffusion along the filaments will show as a less steep decay of the autocorrelation function of fluorescence fluctuations compared to what would be expected from a two-dimensional diffusion. As a result, it can be misinterpreted as a consequence of anomalous subdiffusion. We believe that it would be interesting to address this issue in future experiments and simulations.

As mentioned above, the amphiphilic membrane-targeting sequence, which is used to attach the FtsZ network to the lipid membrane, only inserts into the outer leaflet of a bilayer (23,24). One can therefore pose the question whether the artificial cytoskeleton attached in this manner to the membrane affects the character of phase separation in only the outer leaflet of the GUV or affects both leaflets of the bilayer. In all our experiments, where large-scale phase separation was prevented by the artificial cytoskeleton, we, however, never observed additional large- or intermediate-sized membrane domains with intermediate fluorescence intensity levels, which would indicate

large-scale phase separation in the inner leaflet of the membrane. This suggests that in the system we studied the interleaflet coupling is very strong, synchronizing phase separation in both membrane leaflets.

It has been argued that being singular in nature, the phenomenon of criticality and membrane heterogeneity may not be exploited by biological membranes as they need precise fine tuning (28). On the other hand, our results show that the presence of membrane-interacting components, such as transmembrane proteins, membrane binding proteins, and cytoskeletal elements, can preserve microheterogeneity as well as stabilize fluctuations over a broader range of compositions and temperature, thereby stretching the region where small-scale phase separation (and hence, strong spatial fluctuations) will be observed.

The cellular membrane has multiple ways of interacting with the cytoskeletal components (actin, microtubules, and intermediate filaments). The filaments may directly interact with the membrane or interact with transmembrane or cytoplasmic membrane-binding proteins. Our minimal system illustrates the specific effect of cytoskeletal pinning, in our case, through amphipathic helix insertion, on phase separation. Realistically, all of the aforementioned interactions of cytoskeletal elements with the cell membrane can prevent large-scale phase separation and preserve the membrane microheterogeneity at temperatures above and below the phase transition temperatures.

SUPPORTING MATERIAL

Supporting Materials and Methods and one figure are available at http://www.biophysj.org/biophysj/supplemental/S0006-3495(15)00006-5.

ACKNOWLEDGMENTS

E.P.P. gratefully acknowledges the support from the Deutsche Forschungsgemeinschaft via the Research Unit FOR 877 “From Local Constraints to Macroscopic Transport.”

REFERENCES

1. Arumugam, S., G. Chwastek, and P. Schwille. 2011. Protein-membrane interactions: the virtue of minimal systems in systems biology. *Wiley Interdiscip. Rev. Syst. Biol. Med.* 3:269–280.
2. Klose, C., C. S. Ejsing, …, K. Simons. 2010. Yeast lipids can phase-separate into micrometer-scale membrane domains. *J. Biol. Chem.* 285:30224–30232.
3. Baumgart, T., A. T. Hammond, …, W. W. Webb. 2007. Large-scale fluid/fluid phase separation of proteins and lipids in giant plasma membrane vesicles. *Proc. Natl. Acad. Sci. USA.* 104:3165–3170.
4. Veatch, S. L., P. Cicuta, …, B. Baird. 2008. Critical fluctuations in plasma membrane vesicles. *ACS Chem. Biol.* 3:287–293.
5. Keller, H., M. Lorizate, and P. Schwille. 2009. PI(4,5)P_2 degradation promotes the formation of cytoskeleton-free model membrane systems. *ChemPhysChem.* 10:2805–2812.
6. Ehrig, J., E. P. Petrov, and P. Schwille. 2011. Near-critical fluctuations and cytoskeleton-assisted phase separation lead to subdiffusion in cell membranes. *Biophys. J.* 100:80–89.
7. Machta, B. B., S. Papanikolaou, …, S. L. Veatch. 2011. Minimal model of plasma membrane heterogeneity requires coupling cortical actin to criticality. *Biophys. J.* 100:1668–1677.
8. Witkowski, T., R. Backofen, and A. Voigt. 2012. The influence of membrane bound proteins on phase separation and coarsening in cell membranes. *Phys. Chem. Chem. Phys.* 14:14509–14515.
9. Liu, A. P., and D. A. Fletcher. 2006. Actin polymerization serves as a membrane domain switch in model lipid bilayers. *Biophys. J.* 91:4064–4070.
10. Heinemann, F., S. K. Vogel, and P. Schwille. 2013. Lateral membrane diffusion modulated by a minimal actin cortex. *Biophys. J.* 104:1465–1475.
11. Petrov, E. P., S. Arumugam, …, P. Schwille. 2013. Cytoskeletal pinning prevents large-scale phase separation in model membranes. *Biophys. J.* 104:252A.
12. Honigmann, A., S. Sadeghi, …, R. Vink. 2014. A lipid bound actin meshwork organizes liquid phase separation in model membranes. *eLife.* 3:e01671.
13. Feng, Z. V., T. A. Spurlin, and A. A. Gewirth. 2005. Direct visualization of asymmetric behavior in supported lipid bilayers at the gel-fluid phase transition. *Biophys. J.* 88:2154–2164.
14. Seeger, H. M., G. Marino, …, P. Facci. 2009. Effect of physical parameters on the main phase transition of supported lipid bilayers. *Biophys. J.* 97:1067–1076.
15. Arumugam, S., G. Chwastek, …, P. Schwille. 2012. Surface topology engineering of membranes for the mechanical investigation of the tubulin homologue FtsZ. *Angew. Chem. Int. Ed. Engl.* 51:11858–11862.
16. Arumugam, S., Z. Petrašek, and P. Schwille. 2014. MinCDE exploits the dynamic nature of FtsZ filaments for its spatial regulation. *Proc. Natl. Acad. Sci. USA.* 111:E1192–E1200.
17. Osawa, M., D. E. Anderson, and H. P. Erickson. 2008. Reconstitution of contractile FtsZ rings in liposomes. *Science.* 320:792–794.
18. Dimitrov, D. S., and M. I. Angelova. 1988. Lipid swelling and liposome formation mediated by electric-fields. *Bioelectrochem. Bioenerg.* 19:323–336.
19. Yu, X. C., and W. Margolin. 1997. Ca^{2+}-mediated GTP-dependent dynamic assembly of bacterial cell division protein FtsZ into asters and polymer networks in vitro. *EMBO J.* 16:5455–5463.
20. Honigmann, A., V. Mueller, …, C. Eggeling. 2013. STED microscopy detects and quantifies liquid phase separation in lipid membranes using a new far-red emitting fluorescent phosphoglycerolipid analogue. *Faraday Discuss.* 161:77–89, discussion 113–150.
21. Doube, M., M. M. Kłosowski, …, S. J. Shefelbine. 2010. BoneJ: free and extensible bone image analysis in ImageJ. *Bone.* 47:1076–1079.
22. Ehrig, J., E. P. Petrov, and P. Schwille. 2011. Phase separation and near-critical fluctuations in two-component lipid membranes: Monte Carlo simulations on experimentally relevant scales. *New J. Phys.* 13:045019.
23. Szeto, T. H., S. L. Rowland, …, G. F. King. 2002. Membrane localization of MinD is mediated by a C-terminal motif that is conserved across eubacteria, archaea, and chloroplasts. *Proc. Natl. Acad. Sci. USA.* 99:15693–15698.
24. Szeto, T. H., S. L. Rowland, …, G. F. King. 2003. The MinD membrane targeting sequence is a transplantable lipid-binding helix. *J. Biol. Chem.* 278:40050–40056.
25. Kahya, N., D. Scherfeld, …, P. Schwille. 2003. Probing lipid mobility of raft-exhibiting model membranes by fluorescence correlation spectroscopy. *J. Biol. Chem.* 278:28109–28115.
26. Vequi-Suplicy, C. C., K. A. Riske, …, R. Dimova. 2010. Vesicles with charged domains. *Biochim. Biophys. Acta.* 1798:1338–1347.
27. Dajkovic, A., G. Lan, …, J. Lutkenhaus. 2008. MinC spatially controls bacterial cytokinesis by antagonizing the scaffolding function of FtsZ. *Curr. Biol.* 18:235–244.
28. Bagatolli, L. A., J. H. Ipsen, …, O. G. Mouritsen. 2010. An outlook on organization of lipids in membranes: searching for a realistic connection with the organization of biological membranes. *Prog. Lipid Res.* 49:378–389.